Analytical solution of generalized Burton-Cabrera-Frank equations for growth and post-growth equilibration on vicinal surfaces

S. Harris*
Department of Civil Engineering and Operations Research, Princeton University, Princeton, New Jersey 08544

Pavel Šmilauer†
Interdisciplinary Research Centre for Semiconductor Materials, The Blackett Laboratory, Imperial College, London SW7 2BZ, United Kingdom
(Received 19 May 1994)

We investigate growth on vicinal surfaces by molecular-beam epitaxy making use of a generalized Burton-Cabrera-Frank model. Our primary aim is to propose and implement an analytical program based on a perturbative solution of the nonlinear equations describing the coupled adatom and dimer kinetics. These equations are considered as originating from a fully microscopic description that allows the step boundary conditions to be directly formulated in terms of the sticking coefficients at each step. As an example, we study the importance of diffusion barriers for adatoms hopping down descending steps (Schwoebel effect) during growth and post-growth equilibration of the surface.

I. INTRODUCTION

Growth on vicinal surfaces, with a misorientation angle of a few degrees, is of profound importance as a method of preparing high-quality epitaxial layers and heterostructures.[1] This is also frequently used to obtain insight into the fundamental kinetics of molecular-beam-epitaxy (MBE) growth.[2,3] The renewed interest in the analytical model of Burton, Cabrera, and Frank[4] (BCF) describing epitaxial growth on vicinal surfaces is thus not surprising. In the BCF model, a crystal grows by step propagation due to incorporation of atoms deposited onto the terraces. No interactions between the atoms are considered, and it is also supposed that adatom concentrations at the step edges are at equilibrium and the effect of the step movement can be neglected. This model has been recently generalized for applications pertaining to growth by MBE.[5–9] The far-from-equilibrium character of MBE has led to lifting all of the above restrictions and taking into account the influence of the step movement,[5] deviations from local equilibrium at the step edges,[6] and, finally and most importantly, effects related to lateral interactions of adatoms on the terraces, in particular, formation of adatom islands.[7–9]

Our primary concern in this paper is to propose and carry out an analytical program for solving the generalized BCF equations including nonlinear terms due to adatom interactions. The nonlinear structure of these equations has been the major obstacle to obtaining analytical solutions and for this reason only numerical solutions[7–9] have been reported so far. The steady-state solution of these equations[10] was previously considered through the use of a microscopic formulation based on adatom and dimer position-velocity distribution functions, $f(x,v)$, $\mathcal{F}(x,v)$, instead of the macroscopic densities $m(x)$, $M(x)$ more commonly used,[4,6–9] and we will implicitly use this formulation here as well. However, as discussed below, here this distinction is only operationally significant in the treatment of the boundary conditions which we are able to describe in terms of the step sticking coefficients.

We will assume that the growth conditions (substrate temperature, growth rate, etc.) are such that step flow dominates so that only small islands (dimers) have to be considered, but the step movement is still sufficiently slow so that the steps can be considered stationary in solving the boundary value problem.[7,8] These restrictions are imposed only as simplifications and their removal would increase the complexity and decrease the clarity of our results. All other assumptions introduced in this paper will be clearly noted and assessed in the following sections. While it is our belief that some of these could be eliminated, our main goal here is to obtain a closed-form analytical solution that is based on sound physical and mathematical reasoning.

The outline of this paper is as follows. The necessary equations and notation are presented in Sec. II A where the distinction between the microscopic and macroscopic formulations is made explicit. Our procedure for the solution of these equations then follows in Sec. II B and this is implemented in Sec. III. As a demonstration of our results, we study the effects of barriers to hopping down descending step edges (Schwoebel effect) in Sec. IV. Section V is a brief summary of the results of the paper.

II. THEORETICAL CONSIDERATIONS

A. Basic equations

We consider a stepped crystal substrate on which adatoms are uniformly deposited at a rate Fa^2 where

F is the flux ($m^{-2}s^{-1}$) and a the lattice constant (see Fig. 1). As indicated in the introductory section, the temperature and the flux are supposed to be such that only dimer formation has to be considered but the steps are still sufficiently slow and can be taken as stationary in solving the boundary value problem.[11] Equations describing the evolution of the adatom and dimer densities have been presented and used by several authors.[7–9] These same equations can also be obtained from the microscopic description used by us earlier in treating the steady-state problem[10] if we also assume that the dimers are immobile and that the adatom current is given by Fick's law. The last assumption, which is an integral part of the macroscopic description, is equivalent to neglecting an initial stage in which the current changes over the time scale τ_0 (see below) from zero at the time $t=0$ to the Fick's law value. This should not have a significant qualitative or quantitative impact on our results and therefore seems justified at this juncture of the theoretical development.

Denoting the adatom and dimer densities by $m(x,t)$, $M(x,t)$ to indicate that they are the result from averaging the distribution functions f, $\mathcal{F}$ over velocity, we then have[7,8,10]

$$\frac{\partial m}{\partial t} = D\frac{\partial^2 m}{\partial x^2} + F + 2\gamma M - (8/\tau)m - 2\Gamma m^2, \quad (1)$$

$$\frac{\partial M}{\partial t} = (4/\tau)m + \Gamma m^2 - \gamma M, \quad (2)$$

$$0 \le x \le L\ , \quad t > 0,$$

where D is the diffusion coefficient, $\tau = 1/Fa^2$, $\gamma = \tau_0^{-1}\exp(-E_N/k_BT)$ with the characteristic time for adatom surface diffusion $1/\tau_0 = 2D/a^2 = \nu_0\exp(-E_D/k_BT)$, ν_0 being the attempt frequency, E_N the dimer binding energy and E_D the surface diffusion barrier for a free adatom, and T is the temperature and k_B is the Boltzmann's constant. Also, we have taken the number of dimer-forming sites around a free adatom as four.[9,12]

The terms on the right-hand side of Eq. (1) represent (from left to right): diffusion of free adatoms, deposition of an atom on a surface site with all nearest-neighbor positions unoccupied, dimer breakup, dimer formation due to direct collision of an atom from the beam with a surface adatom, and dimer formation when two diffusing adatoms meet each other (cf. Fig. 1). The prefactor $\Gamma = \sigma a^2/\tau_r$ with σ the capture efficiency which we subsequently set to unity,[7] combines a geometrical factor σa^2 and a relaxation time that we have denoted as τ_r. In previous numerical studies[7–9] $\tau_r = \tau_0$ has been used; here we will use $\tau_r = (FD)^{-1/2}$, which is a considerably larger quantity. It can be shown[13] that $\tau_r = (FD)^{-1/2}$ is in quantitative agreement with Eqs. (1), (2) while $\tau_r = \tau_0$ is not. Separate justifications based on kinetic arguments have also been given in the literature.[14]

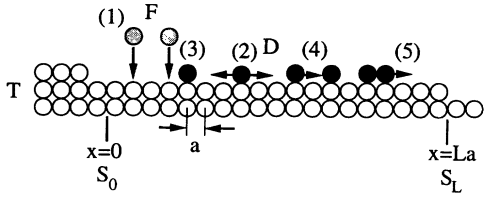

FIG. 1. Schematic picture of the processes considered in our model. Atoms are deposited (1) at a rate F onto the substrate with a lattice constant a held at a temperature T. They migrate (2) with the diffusion coefficient D and attach either to the preexisting steps (with probabilities given by the sticking coefficients S_0 and S_L) or form dimers (3), (4), which can subsequently disassociate (5). Two ways of a dimer creation, by a deposition of an incoming atom onto a nearest-neighbor site of a surface adatom (3) or by an encounter of two migrating adatoms (4), are shown.

The initial conditions for Eqs. (1), (2) are $m(x,0) = M(x,0) = 0$, i.e., the beam is initiated at $t=0$ at which time the terraces are unoccupied. So far there is no difference between our description, Eqs. (1), (2) with the above initial conditions, and the macroscopic descriptions cited earlier.[7–9] However, in specifying the boundary conditions the advantages of the microscopic theory become clear and a major difference between the two approaches emerges. At the level of approximation in the microscopic theory[10,15] leading to the above kinetic equations, the distribution function f describing the adatoms is given as

$$f(x,v,t) = \{m_1(x,t)\Theta(v) + m_2(x,t)[1-\Theta(v)]\}(2\pi\alpha)^{-1/2}e^{-v^2/2\alpha}, \quad (3)$$

where $\Theta(v)$ is the standard Heaviside function and $\alpha = k_BT$ (the adatom mass is expressed in units in which it is unity). This leads to

$$m = (m_1+m_2)/2\ ,\ j = -D\frac{\partial m}{\partial x} = (\alpha/2\pi)^{1/2}(m_1-m_2). \quad (4)$$

It follows from Eqs. (3) and (4) that m_1 is the density of adatoms moving with positive velocity on the terrace and m_2 the density of those moving with negative velocity. This level of detail is particular to the microscopic description and allows us to prescribe natural boundary conditions. The most general of these, which we use here, is given in terms of the step sticking coefficient S_i, $i=0,L$ for $x=0,L$, respectively (Fig. 1). For asymmetric step conditions at $x=0,L$

$$S_0 = [m_2(0) - m_1(0)]/m_2(0)\ ,$$
$$S_L = [m_1(L) - m_2(L)]/m_1(L)\ , \quad (5)$$

with $0 \le S_i \le 1$. The finite parameters S_i describe the full range of step conditions from blocking ($S_i = 0$) to total absorption ($S_i = 1$). In addition to the conceptual advantage in using the microscopic boundary condition there is also an operational advantage. From Eq. (4) we find

$$-h_L m = \frac{\partial m}{\partial x}\ ,\quad x=L \quad (6a)$$

$$h_0 m = \frac{\partial m}{\partial x}\ ,\quad x=0, \quad (6b)$$

with $h_i = [S_i/D(2-S_i)](2\alpha/\pi)^{1/2}$. Thus, for the full range of step kinetics the boundary condition is of the Neumann (or radiation) type and a single solution depending on the S_i describes all possible sticking conditions. Equations (1), (2), and (6) together with the initial conditions define the problem to be considered in mathematical terms. Note that there is no boundary condition for M required for the case considered of slow steps and fixed dimers. In the steady state an exact solution for these equations was obtained[10] despite their nonlinearity; here we cannot expect to be so fortunate and therefore we have to look for an approximate means of solution.

B. Plan of solution

We propose to solve the problem defined above by tailoring a procedure of solution to our intuitive expectation of how the physical process evolves. Initially the terraces are unoccupied, adatoms are deposited and begin to diffuse to the steps and, as their density increases, dimers begin to be formed and, finally, the latter may begin to disassociate. Thus, three separate evolutionary stages, most likely not sharply defined, are suggested. One mathematical interpretation of this is to consider the terms in Eq. (1) representing dimer effects to be of higher order in an approximation scheme; M also will be of higher order. Writing $m = m^{(0)} + m^{(1)} + \cdots$, $M = M^{(1)} + M^{(2)} + \cdots$ and rewriting Eq. (1) we have

$$\frac{\partial m}{\partial t} = D\frac{\partial^2 m}{\partial x^2} + F - R(m, M), \tag{1'}$$

$$\frac{\partial M}{\partial t} = \frac{1}{2}R(m, M). \tag{2'}$$

[$R(m, M)$ represents all the terms on the right-hand side of Eq. (1) which are not given explicitly] so that our procedure for solution is implemented by considering the following equations:

$$\frac{\partial m^{(0)}}{\partial t} = D\frac{\partial^2 m^{(0)}}{\partial x^2} + F, \tag{7}$$

$$\frac{\partial m^{(1)}}{\partial t} = D\frac{\partial^2 m^{(1)}}{\partial x^2} - R(m^{(0)}, 0), \tag{8}$$

$$\frac{\partial M^{(1)}}{\partial t} = \frac{1}{2}R(m^{(0)}, M^{(1)}), \ldots, \tag{9}$$

with, e.g.,

$$h_0 m^{(0)} = \frac{\partial m^{(0)}}{\partial x}\ , \quad h_0 m^{(1)} = \frac{\partial m^{(1)}}{\partial x}, \ldots, x = 0. \tag{10}$$

The connection between the preceding physical and mathematical descriptions becomes clearer if we operate on Eq. (1) with $\partial/\partial t$ and use Eq. (2) to obtain

$$\frac{\partial}{\partial t}\left[\frac{\partial m}{\partial t} - D\frac{\partial^2 m}{\partial x^2} - F\right] = -\gamma\left[\frac{\partial m}{\partial t} - D\frac{\partial^2 m}{\partial x^2} - F\right] - \frac{\partial}{\partial t}[8m/\tau + 2\Gamma m^2] \tag{11}$$

$$\equiv -R_1(m) - \frac{\partial R_2(m)}{\partial t}. \tag{1''}$$

The first term on the right-hand side is the contribution due to dimer breakup, indicated by the γ prefactor, while the second is the contribution due to dimer formation. Since $R_1(m^{(0)}) = 0$ by virtue of Eq. (7) and $\partial R_2(m^{(0)})/\partial t \neq 0$ we see that the mathematical description given by Eqs. (7), (8) reflects our conjectured physical picture in which dimer breakup effects are of higher order than dimer formation effects. In lowest order the right-hand side of Eq. (11), which contains only dimer effects, is set equal to zero and the left-hand side is used to determine $m^{(0)}$, which identically recovers Eq. (7) since $\partial F/\partial t = 0$, $\partial m^{(0)}(x,0)/\partial t = F$, $\partial^2 m^{(0)}(x,0)/\partial x^2 = 0$ so that

$$\frac{\partial}{\partial t}\left[\frac{\partial m^{(0)}}{\partial t} - D\frac{\partial^2 m^{(0)}}{\partial x^2} - F\right] = \frac{\partial}{\partial t}\left[\frac{\partial m^{(0)}}{\partial t} - D\frac{\partial^2 m^{(0)}}{\partial x^2}\right] = 0 \tag{12a}$$

and

$$\frac{\partial m^{(0)}(x,t)}{\partial t} = D\frac{\partial^2 m^{(0)}(x,t)}{\partial x^2} + F. \tag{12b}$$

In what follows we will directly use Eqs. (7) and (8) to determine $m^{(0)}$, $m^{(1)}$.

The preceding discussion contains a rationale, based on physical reasoning, together with a supporting mathematical argument, for implementing a perturbative approximation of Eqs. (1'), (2'). Our reasoning here is admittedly heuristic, however given the intractable nature of reaction-diffusion equations in general (a bounded domain is the most difficult case), we believe that the approach outlined above is a reasonable first step in obtaining a useful analytical solution for the generalized BCF equations in the regime near step flow where dimer effects begin to play a role. It has been shown[8] that in this regime the moving boundary effect can still be neglected so that this omission here is not an issue. It is possible that the procedure outlined above could be formalized through the use of a scaling argument leading to the introduction of one or more parameters of smallness; we have not attempted to do this here since the underlying physical rationale is so intuitively appealing and transparent. In the next section we obtain explicit results for $m^{(0)}$, $m^{(1)}$, and $M^{(1)}$ by implementing the program described above.

III. SOLUTIONS

A. Lowest order; $m^{(0)}$

As discussed above, we write $m = m^{(0)} + m^{(1)} + \ldots$ and determine $m^{(0)}$, $m^{(1)}$ from Eqs. (7), (8) together with the boundary conditions specified by Eq. (10). These equations can be solved by standard methods;[16] we first consider the equation for $m^{(0)}$, Eq. (7) for the general case where the beam F is turned off at $t = t^*$. The exact solution for $t < t^*$ is

$$m^{(0)}(x,t) = \sum_{n=1}^{\infty}(F/Db_n^2)(1-e^{-b_n^2 Dt}) \times K(b_n,x)\int_0^L K(b_n,x')dx', \tag{13}$$

where the eigenfunctions $K(b_n,x)$ are[15]

$$K(b_n,x) = \sqrt{2}\,[b_n\cos b_n x + h_0 \sin b_n x] \times[(b_n^2+h_0^2)(L+h_L(b_n^2+h_L^2)^{-1}+h_0)]^{-1/2}, \tag{14}$$

and the eigenvalues b_n are given by the positive roots of $b(h_0+h_L) = (b^2 - h_0h_L)\tan bL$. The terms without the exponential factor can be directly summed but the tedious algebraic manipulation required can be avoided by noting that these terms are the nondecaying part of the solution, i.e., the steady-state solution of Eq. (7). In order to simplify the remaining sum and obtain a result that is both easier to use and also makes the next level of approximation tractable we will replace b_n, *in the exponential term only*, by a lumped eigenvalue, b.[17] In Sec. III D we indicate a procedure for determining b in terms of the system parameters through the imposition of a consistency constraint.

Making the above simplification we then have

$$m^{(0)}(x,t) = (F/2DA_0)(-A_0x^2 + h_0B_0x + B_0)\mathcal{F}_0(t), \tag{15}$$

where

$$A_0 = h_0 + h_L + h_0h_LL, \tag{16a}$$
$$B_0 = 2h_0L + h_0h_LL^2, \tag{16b}$$
$$\mathcal{F}_0(t) = \begin{cases} 1-e^{-b^2Dt}\,, & t<t^* \quad (16c)\\ e^{-b^2D(t-t^*)} - e^{-b^2Dt}\,, & t>t^*. \quad (16d)\end{cases}$$

The above results can be nondimensionalized (see the Appendix) but for now it is most convenient to retain the dimensional form shown above.

B. First order: Adatom density $m^{(1)}$

The equation for $m^{(1)}$ is given from Eq. (8) as

$$\frac{\partial m^{(1)}}{\partial t} - D\frac{\partial^2 m^{(1)}}{\partial x^2} = -(8/\tau)m^{(0)} - 2\Gamma(m^{(0)})^2 = R_2(m^{(0)}). \tag{17}$$

This equation is a more general version of Eq. (7), i.e., a diffusion equation with a source term that here is not constant but depends on both space and time. The formal solution is

$$m^{(1)} = \sum_{n=1}^{\infty} e^{-b_n^2Dt}K(b_n,x)\int_0^t dt' e^{b_n^2Dt'}\int_0^L dx' K(b_n,x')R_2(m^{(0)}(x',t')). \tag{18}$$

We denote the contribution from that part of R_2 linear in $m^{(0)}$ as $m^{(11)}$ so that $m^{(1)} = m^{(11)} + m^{(12)}$; further we note that $m^{(11)}$ will be identically zero when the beam is turned off. Using Eq. (15) for $m^{(0)}$ and again replacing b_n by b in the exponential terms after the t' integration is carried out, we find

$$m^{(11)}(x,t) = \frac{4F}{\tau D^2A_{11}}\left(\frac{-A_{11}}{12}x^4 + \frac{h_0B_{11}}{6}x^3 + \frac{B_{11}}{2}x^2 + \frac{C_{11}h_0}{A_{11}}x + \frac{C_{11}}{A_{11}}\right)\mathcal{F}_{11}(t), \tag{19}$$

where

$$A_{11} = A_0\,,\quad B_{11} = B_0, \tag{20a}$$

$$C_{11} = \left[\frac{A_0h_L}{12}L^4 + \left(\frac{A_0}{3} - \frac{h_0h_LB_0}{6}\right)L^3 - \left(\frac{h_LB_0}{2} + h_0B_0\right)L^2 - B_0L\right], \tag{20b}$$

$$\mathcal{F}_{11}(t) = [(1-e^{-b^2Dt}) - b^2Dt\,e^{-b^2Dt}][1-\Theta(t^*)]. \tag{20c}$$

The contribution from that part of R_2 nonlinear in $m^{(0)}$, denoted previously as $m^{(12)}$, is obtained from Eq. (18). Making use again of the simplification introduced earlier we obtain

$$m^{(12)}(x,t) = -2\Gamma\left(\frac{F}{2DA_{12}}\right)^2\left[\frac{A_{12}^2}{30}x^6 - \frac{h_0A_{12}B_{12}}{10}x^5 + \frac{(h_0B_{12})^2 - 2A_{12}B_{12}}{12}x^4 + \frac{h_0B_{12}^2}{3}x^3 + \frac{B_{12}^2}{2}x^2 + \frac{h_0C_{12}}{A_{12}}x + \frac{C_{12}}{A_{12}}\right]\mathcal{F}_{12}(t), \tag{21}$$

where

$$A_{12} = A_0\,,\quad B_{12} = B_0 \tag{22a}$$

$$C_{12} = h_L\left\{-\frac{A_{12}^2}{30}L^6 + \left(\frac{A_{12}B_{12}h_0}{10} - \frac{A_{12}^2}{5h_L}\right)L^5 - \frac{1}{12}\left[(h_0B_{12})^2 - 2A_{12}B_{12} - \frac{6A_{12}B_{12}h_0}{h_L}\right]L^4 - \frac{1}{3}\left[h_0B_{12}^2 + \frac{(h_0B_{12})^2}{h_L} - 2A_{12}B_{12}\right]L^3 - \left[\frac{h_0B_{12}^2}{h_L} + \frac{B_{12}^2}{2}\right]L^2 - \frac{B_{12}^2}{h_L}L\right\}, \tag{22b}$$

$$\mathcal{F}_{12}(t) = \begin{cases} [1-e^{-2b^2Dt}] - 2b^2Dt\,e^{-b^2Dt}\,, & t<t^* \quad (22c)\\ 2e^{-b^2D(t-t^*)} - 2b^2Dt^*\,e^{-b^2Dt} \\ -[e^{-2b^2D(t-t^*)} + e^{-2b^2Dt} \\ +2(e^{-b^2Dt} - e^{-b^2D(2t-t^*)})]\,, & t>t^*. \quad (22d)\end{cases}$$

C. First order: Dimer density $M^{(1)}$

In a first approximation the dimer density is found from Eq. (9); although this equation includes disassociation effects these do not contribute directly to the solution which is consistent with the logic underlying the approximation procedure we are using.[18] The initial condition for Eq. (9) is $M^{(1)}(x,0) = M(x,0) = 0$, so that the direct contribution of the disassociation term $\gamma M^{(1)}$ vanishes and we obtain

$$M^{(1)} = \frac{1}{2}\int_0^t dt' e^{-\gamma(t-t')}[4m^{(0)}(x,t')/\tau + \Gamma(m^{(0)}(x,t'))^2] \tag{23}$$

so that $M^{(1)}$ is given directly from Eq. (15) following a simple integration. If we write $m^{(0)} = m^{(0)}(x)\mathcal{F}_0(t)$ then, in a notation identical to that used for indicating the separate contributions to $m^{(1)}$,

$$M^{(11)} = 2(m^{(0)}(x)/\tau)\mathcal{F}_{21}(t), \tag{24}$$

$$\mathcal{F}_{21}(t) = \begin{cases} \gamma^{-1}(1-e^{-\gamma t}) - (\gamma - b^2 D)^{-1}(e^{-b^2 D t} - e^{-\gamma t}) , & t < t^* \quad (25a) \\ \gamma^{-1}(e^{-\gamma(t-t^*)} - e^{-\gamma t}) - (\gamma - b^2 D)^{-1}(e^{-b^2 D t} e^{-\gamma(t-t^*)} - e^{-\gamma t}) , & t > t^*, \quad (25b) \end{cases}$$

$$M^{(12)} = \Gamma(m^{(0)}(x))^2 \mathcal{F}_{22}(t) \tag{26}$$

$$\mathcal{F}_{22}(t) = \begin{cases} \gamma^{-1}(1-e^{-\gamma t}) - 2(\gamma - b^2 D)^{-1}(e^{-b^2 D t} - e^{-\gamma t}) + (\gamma - 2b^2 D)^{-1}(e^{-2b^2 D t} - e^{-\gamma t}) , & t < t^* \quad (27a) \\ \gamma^{-1}(e^{-\gamma(t-t^*)} - e^{-\gamma t}) - 2(\gamma - b^2 D)^{-1}(e^{-b^2 D t^*} e^{-\gamma(t-t^*)} - e^{-\gamma t}) \\ -(\gamma - 2b^2 D)^{-1} e^{-\gamma t} + (\gamma - 2b^2 D)^{-1}[e^{-2b^2 D(t-t^*)} - e^{-\gamma(t-t^*)} + e^{-2b^2 D t} \\ -2e^{-b^2 D(2t-t^*)} + 2e^{-b^2 D t^*} e^{-\gamma(t-t^*)}] , & t > t^*. \quad (27b) \end{cases}$$

D. Determination of the lumped eigenvalue b

The major approximation we have made is replacing b_n by b in Eq. (13) which is the basis for Eqs. (15), (19), and (21). It would be possible to use a second lumped eigenvalue in the calculations used in obtaining the latter two results, but this would appear to overcomplicate matters at this point. What is important for our present purposes is the prescription of a rule that fixes b in terms of the system parameters. The basis for such a rule is a consistency requirement that the value of the coverage as determined from Eqs. (1), (2), and (6) be identical with that found directly from their solution; we show how this can be done using the zeroth-order approximation.

If we determine the coverage by directly integrating the solution, $m^{(0)}$, we find

$$\begin{aligned} \Theta(t) &= \int_0^L m^{(0)}(x,t), dx \\ &= (FL^2/12D)\left[4L(h_0+h_L) + h_0 h_L L^2 + 12\right] \\ &\quad \times (h_0 + h_L + h_0 h_L L)^{-1} \mathcal{F}_0(t). \end{aligned} \tag{28}$$

Using Eqs. (1) and (6), after integrating the former we find

$$\frac{\partial \Theta}{\partial t} = FL + D[-h_L m^{(0)}(L,t) - h_0 m^{(0)}(0,t)] \tag{29}$$

from which it follows that

$$\Theta(t) = (FL/b^2 D)\mathcal{F}_0(t) \tag{30}$$

and then

$$b^{-2} = (L/12)[4L(h_0+h_L) + h_0 h_L L^2 + 12]\,(h_0 + h_L + h_0 h_L L)^{-1}. \tag{31}$$

E. Discussion

Before considering some numerical consequences of the above solutions, which we do in the next section, it is best to add here a few final comments pertaining to the procedure followed in obtaining these. The approximation procedure is *ad hoc* and follows from physical reasoning supported by the consistency of the resulting mathematical formulation. Although we have only considered the first approximation beyond the step-flow solution, in principle higher-order corrections could be obtained. It appears to be more useful to consider instead additional effects due to moving steps and larger islands in the present context. The former of these appears to be tractable, and we hope to be able to report on this in a future study. Finally, we want to emphasize that the procedure used here is distinct from standard methods based on linearization or a formal small parameter expansion and in our opinion captures the essence of physical processes that are taking place better than either of these methods.

IV. EXAMPLE APPLICATION: SCHWOEBEL EFFECT DURING GROWTH AND POST-GROWTH RECOVERY

A. Surface roughness and its evolution during growth and post-growth equilibration of the surface

The roughness of growing surfaces has become one of the main topics of interest in the study of surface processes. One reason for this is the evident importance of minimizing surface roughness for applications, e.g., for the deposition of narrow layered structures (quantum wells, lateral superlattices, magnetic multilayers, etc.) required for the fabrication of devices such as quantum well lasers or modulation-doped field effect transistors. The performance of such devices depends critically on the morphological quality of epitaxial layers and interfaces.

Another reason for the intense interest in surface roughness is purely theoretical. The roughness of growing surfaces has been observed to exhibit asymptotic dynamical scaling behavior which has led to the classification of growth models into various universality classes. In a majority of the theoretical studies, the focus has been on the evolution of the surface morphology due to fluctuations in the incoming flux of particles and surface diffusion. However, recently the influence of additional activation barriers to adatom hopping between layers [the Schwoebel effect (SE), Refs. 19 and 20] on the developing surface roughness has been studied by Villain[21] and identified as a cause of an intrinsic growth instability on nominally flat surfaces. On vicinal surfaces, the additional step-edge barriers to hopping down descending steps stabilize growth and lead to equalization of terrace widths.[20,21]

From a practical point of view, the growth interruption technique[22] has become a useful method for obtaining atomically abrupt interfaces during growth by MBE. In this technique, growth is briefly interrupted by stopping the cation (but not the anion) flux. After the growth is stopped, the surface smoothes which causes the recovery of the specular-beam intensity of the commonly used monitoring probe, reflection high-energy electron-diffraction (RHEED), to its initial pregrowth value. It has been found experimentally that the recovery of the intensity $I(t)$ can be fitted by an empirical expression[23]

$$I(t)=A_0+A_1e^{-t/\tau_1}+A_2e^{-t/\tau_2}\ ,\quad t>t^*, \tag{32}$$

where A_0, A_1, and A_2 are constants, and τ_1 and τ_2 are the time constants for the fast and slow stages of recovery, respectively. The time constant of the initial stage of recovery, τ_1, has been shown to have a strong systematic dependence both on the substrate temperature and on the point in layer completion at which growth is interrupted.[23]

The recovery process is also of profound theoretical importance. The equilibration of a surface after a period of growth is a more discriminating test of theoretical models than growth alone. During growth under typical conditions, the maximum time scale is set by the deposition flux and processes occurring over longer time scales are "frozen out." However, during recovery, these processes can come into play even though their effect during growth can be safely omitted.[24] Indeed, Monte Carlo (MC) simulation studies which yielded very good results when directly compared to observed behavior during growth, appeared to be unable to reproduce the recovery curves, in particular at low temperatures, where no temperature dependence of τ_1 was observed in simulations.[3] Similarly, the detailed study of the recovery process by Vvedensky and Clarke[24] using the same MC model showed that in their simulations there was no relevant dependence of τ_1 on the point where growth was interrupted.

Peng and Whelan[25] suggested that interlayer transport is of key importance for the correct reproduction of the behavior of τ_1. However, large values of τ_1 observed in experiment can be explained only if there is some mechanism hindering interlayer transport. The obvious choice for such a mechanism is the SE, and recent simulations[26] have shown that it indeed results in slowing down the recovery process. However, it has been also found that the SE alone cannot explain the observed behavior and an additional process must be introduced in which a freshly arrived atom is incorporated at a site with the highest number of nearest neighbors in a certain region around the initial site of incidence.[26] This incorporation scheme results in smoother edges of both preexisting steps and adatom islands. An independent proof exists that such a change in the model leads to a better reproduction of the post-deposition recovery. In Ref. 8, the authors had to consider detachment of atoms from steps and breakup of islands composed of up to ten atoms in order to obtain good qualitative agreement with the experimentally observed behavior. Significantly, they assumed a shape for each island that is as close as possible to a square (i.e., very compact and with smooth edges). Similarly, the breakup of the most stable configurations has been found to be a crucial step for the post-growth relaxation of the surface in Ref. 27.

MC simulations which included both the SE and the smoothing due to the incorporation have led to *quantitative* agreement with the experimental data[26] which is strong circumstantial evidence for the existence of the Schwoebel barriers on a GaAs(001) surface. Additional evidence has been provided in a recent paper by Johnson *et al.*[28] who observed (using scanning tunneling and atomic force microscopies) growth instability and formation of large mounds on a nominally flat GaAs(001) surface. Finally, a recent analysis[29] of the RHEED data of Ref. 3 demonstrated that sticking coefficients at ascending and descending steps on GaAs(001) surfaces are indeed strongly asymmetric providing further support for the existence of the step-edge barriers on this surface.

In light of the above, it would be interesting to study the influence of the SE using the analytical results presented above and taking advantage of the natural treatment of the boundary conditions. We will use the parameters used for simulations of GaAs(001) growth and try to make a comparison to some of the experimental results of Ref. 3.

B. Adatom and dimer concentration profiles and densities, the surface step density, and their time evolution

In this section, we discuss adatom and dimer concentration profiles, and the time evolution of the total densities of adatoms and dimers and of the surface step density, during deposition and after its cessation. We study both the case with and without the SE (i.e., with different and equal sticking coefficients at boundaries of the terraces, respectively). Note that the nondimensionalized form of the equations has been used in numerical evaluation of the equations, cf. Sec. III and the Appendix.

In our calculations, we proceeded with "deposition" until the saturation of the total density of adatoms and dimers on the terraces (i.e., a steady-state situation) has been achieved, see Fig. 3, and then we interrupted it. The terrace width L has been chosen to be 20 lattice constants. The sticking coefficient at the *ascending* step (S_0 in Fig. 1) has been estimated based on the dimer binding energy E_N (assuming straight steps similar to Myers-Beaghton and Vvedensky in Ref. 8, Sec. IV B), as $S_i = 1 - \exp(-E_N/k_BT)$, whereas the sticking coefficient at the *descending* step (S_L in Fig. 1) was estimated using the additional step-edge barrier height E_B as well, $S_i = \exp(-E_B/k_BT) - \exp(-E_N/k_BT)$. The values of parameters $E_D = 1.54$ eV [which determines the diffusion coefficient D, see the paragraph following Eq. (2) in Sec. II A], $E_N = 0.231$ eV, and $E_B = 0.175$ eV were taken from the results of the fitting procedure in Ref. 26. The attempt frequency ν_0 has been calculated from $\nu_0 = 2k_BT/h$, where h is the Planck's constant. The value of the flux F was 0.20 ML/s, and the values of the substrate temperature T are given in the figures.

Adatom and dimer concentration profiles shown in Fig. 2 have been calculated at the time t^* when the deposition was stopped (in the saturation region). The upper two panels (a and b) of Fig. 2 are for the case without the SE, whereas the lower two (c and d) are for the case with the SE. The panels a and c show both the total adatom density m (solid lines) and the adatom density in the lowest order of approximation, $m^{(0)}$ (dotted lines), cf. Eqs. (15) and (16).

The profiles for the case with the SE are asymmetric and exhibit a maximum near the reflecting boundary. Notice that significantly higher adatom and dimer densities build up on the terraces due to the presence of the Schwoebel barriers. It is also interesting to mention that whereas the densities with and without the SE are of approximately the same order of magnitude just after the growth is stopped (Fig. 2) they differ by many orders of magnitude after the equilibration due to a larger time constant for this process in the case with the SE (see below). Note also that concentration profiles do not vanish at boundaries, $x = 0, 1$ (in contrast to those in Refs. 7 and 30) due to the microscopic treatment of the boundary conditions in our approach, cf. Sec. II A.

In Fig. 3, the time evolution of the total densities of adatoms and dimers on terraces is shown. The strong temperature dependence of the densities and of the difference between m and $m^{(0)}$ can be again observed. However, the most significant difference is a rather drastic change of the time for the decay of the adatom and dimer densities due to the SE. This confirms that the inclusion of the barriers to hopping at step edges does lead to a slower relaxation of the surface after growth is terminated, a conclusion reached previously in the MC study mentioned above.[26]

Finally, in Fig. 4, the evolution of the surface step density calculated in a pseudo-two-dimensional approximation (similar to that used in Ref. 8) is shown. For the calculation of this quantity, we supposed that every free adatom and dimer contributes four and six steps, respectively. The panel a shows the results without the SE, whereas the panel c those with the SE. The experimental results at similar temperatures taken from Ref. 3 (RHEED specular-beam intensity during the post-growth recovery on a GaAs(001) vicinal surface misoriented by 2° toward the [010] direction) are shown in the panel b. Notice the order of magnitude difference in the time scale which is discussed in the following section.

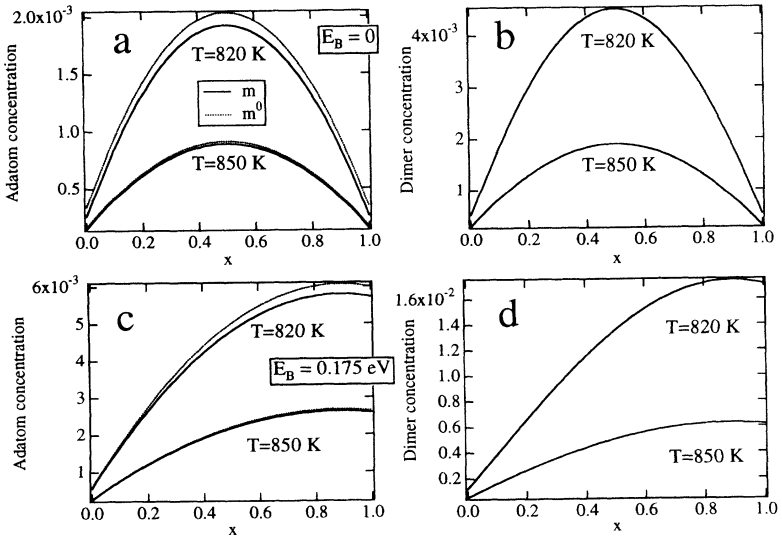

FIG. 2. Adatom (a, c) and dimer (b, d) concentration profiles immediately after growth is stopped at the steady-state region. The panels a, b and c, d show the results obtained without and with the Schwoebel effect, respectively. See text for more details.

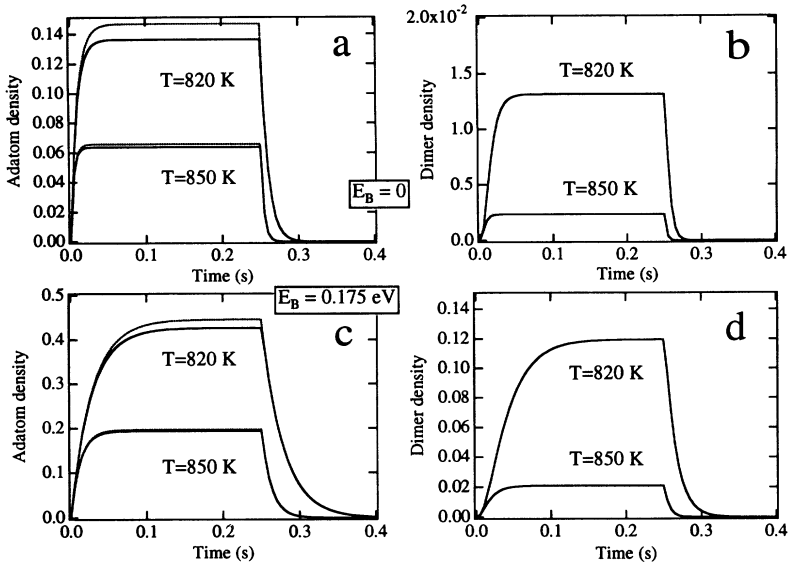

FIG. 3. Time evolution of adatom (a, c) and dimer (b, d) densities. The panels a, b and c, d show the results obtained without and with the Schwoebel effect, respectively.

C. Discussion

The above numerical results are based on evaluation of the preceding analytical results and agree with earlier numerical studies.[7–9,30] The advantage of our approach (besides the important fact that we were able to obtain analytic formulas) is the microscopic level of the description of the growth process and resulting natural treatment of boundary conditions. We have demonstrated than even a relatively small Schwoebel barrier has a profound influence on behavior during growth and, in particular, during the post-growth recovery. Another detail worth mentioning is that had we used τ_0 instead τ_r for the time constant in the prefactor Γ in Eq. (2) (see the discussion in Sec. II A), the contribution $m^{(12)}$ to the adatom density would be underestimated by several orders of magnitude. Let us now discuss several problems related to our results.

As expected, the difference between the adatom concentration profiles obtained using formulas for m and $m^{(0)}$ [Figs. 2(a), 2(c)] is not important under conditions near the step-flow growth mode (the biggest difference being observed near the maxima), but increases as the temperature is decreased (cf. similar results in Fig. 1 of Ref. 30). However, this does not mean that the dimer (and larger islands) formation is not important. It was shown by Stoyanov[31] and Myers-Beaghton and Vvedensky[7] that adatom interactions lower the adatom diffusivity by several orders of magnitude and, if not taken into account properly (as is the case when the Einstein relation for surface diffusion $x^2 = 2Dt$ is used[2]), lead to an estimate of the critical temperature T_c (at which growth starts to proceed via step flow) which is incorrect by up to 200 K.[7] In other words, whereas the

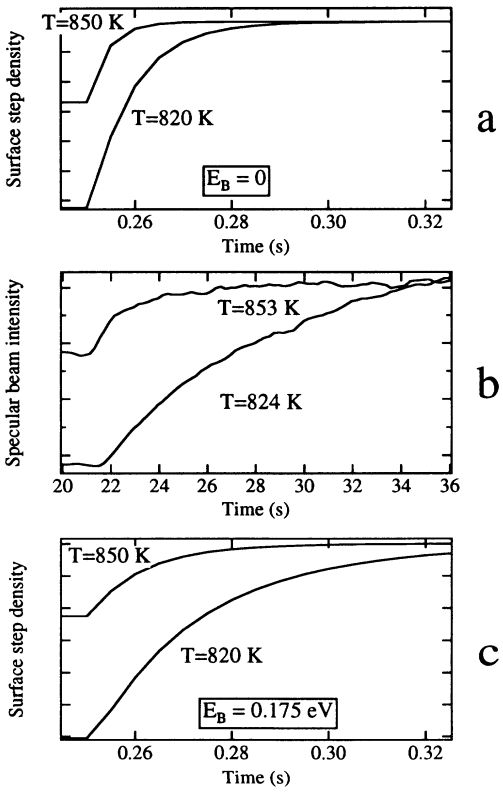

FIG. 4. Time evolution of the surface step density (panels a, c) and the RHEED specular beam intensity (b). The panels a and c show the results obtained without and with the Schwoebel effect, respectively. The direction of vertical axis in the plots of the step density is reversed to allow for comparison with the RHEED specular-beam intensity (see Refs. 3 and 26), i.e., the step density increases *downwards*.

concentration profiles can be calculated in the lowest order of approximation near T_c, the critical temperature itself must be determined taking higher-order effects into account.

The time constants for the post-growth recovery of the adatom and dimer densities are an order of magnitude smaller than observed in experiment (cf. Fig. 3 and particularly Fig. 4). This is not surprising given the fact that in our model, the effect of breakup of larger islands is not taken into account. It was convincingly demonstrated by Myers-Beaghton and Vvedensky[8] and Kenny *et al.*[27] how significant these processes are for the correct reproduction of the recovery curves, and this process was also shown to be important in the MC study mentioned above[26] where it was found that step and island edges smoothed by the incorporation mechanism of the incoming atoms (see above) act in concert with the step-edge barriers to slow down the recovery process. Also the fact that one-dimensional diffusion in our model leads to more rapid changes of the surface adatom population as compared to the two-dimensional case adds to the difference in the speed of surface smoothing.

Finally, in the framework of our simple model, we cannot observe oscillations of the density of adatoms, dimers, or the surface step density (or oscillations of related quantities like the specular-beam intensity of some diffraction probe calculated in the kinematic approximation). Such oscillations are not experimentally observed near the step-flow growth mode where our model is, strictly speaking, only supposed to be valid. However, it is possible to obtain oscillations at lower temperatures (or higher fluxes) even in this class of models provided the step movement is taken into account.[8] As we already mentioned, the inclusion of this effect into our perturbative scheme seems to be possible (cf. Sec. I).

V. SUMMARY

In summary, we have investigated epitaxial growth on vicinal (stepped) surfaces using an analytical program based on a perturbative solution of the generalized Burton-Cabrera-Frank equations. The nonstandard scheme followed by us is motivated by physical insight into the growth process. This approach allowed us to obtain closed-form analytical solutions for the adatom and dimer densities while using a microscopic description of the boundary conditions. The scheme is open to further improvements and inclusion of other effects such as the movement of the preexisting steps.

We applied the analytical results to the study of the influence of the Schwoebel effect (additional barriers to interlayer hopping at step edges) on the evolution of adatom and dimer populations and of the surface step density during growth and post-growth equilibration of the surface and compared them (where it was possible) to the experimental results. The Schwoebel effect was shown to have a significant impact on the behavior during growth and, in particular, during the post-growth recovery, but it has also become apparent that larger islands and their decay have to be taken into account if the recovery curves obtained experimentally and in simulations are to be reproduced. In order to obtain a more realistic description of the growth process at lower temperatures (including oscillations of step density or kinematic intensity), additional processes must be considered such as the above-mentioned step movement.

ACKNOWLEDGMENTS

The NATO Travel Grant No. CRG 931508, and the support of Imperial College and the Research Development Corporation of Japan under the auspices of the "Atomic Arrangement: Design and Control for New Materials" Joint Research Program are gratefully acknowledged. S.H. also thanks the Department of Civil Engineering and Operations Research at Princeton University for their hospitality.

APPENDIX: DIMENSIONLESS VARIABLES

It is convenient for the purposes of assessing the effects of various parameters to represent the results obtained in dimensionless form. Introducing $x' = xL$ and $(h_i)' = ah_i$ and using the relationships $D = a^2/2\tau_0$, $a/\tau_0 = \sqrt{2\alpha}$ which provide reasonable estimates, we then find, e.g., for $m^{(0)}$

$$a^2 m^{(0)} = (\tau_0/\tau A_0)[-A_0(L/a)^2 x^2 + h_0 B_0 (L/a)x + B_0]\mathcal{F}_0(t), \tag{A1}$$

where we have dropped the primes for notational convenience. Now $0 \le x \le 1$ and

$$h_i = [S_i/(2 - S_i)]\,(2/\sqrt{\pi}), \tag{A2}$$

$$A_0 = h_0 + h_1 + h_0 h_1 (L/a), \tag{A3}$$

$$B_0 = h_1 (L/a)^2 + 2(L/a), \tag{A4}$$

and

$$1/Db^2 = (L/a)\,(\tau_0/6A_0)\,[4(L/a)(h_0 + h_1) + h_0 h_1 (L/a)^2 + 12]. \tag{A5}$$

Similar results follow for $m^{(1)}$ and $M^{(1)}$ but because they are so lengthy we do not include them here.

---

* Also at Interdisciplinary Research Centre for Semiconductor Materials, The Blackett Laboratory, Imperial College, London SW7 2BZ, United Kingdom; present address: College of Engineering and Applied Sciences, SUNY, Stony Brook, NY 11794.

† Also at Department of Physics, Imperial College, London SW7 2BZ, United Kingdom; on leave from Institute of Physics, Cukrovarnická 10, 162 00 Praha 6, Czech Republic.

[1] M. Tanaka and H. Sakaki, Jpn. J. Appl. Phys. **27**, L2025

(1988), Pt. 2; M. Tsuchiya, J.M. Gaines, R.H. Yan, R.J. Simes, P.O. Holtz, L.A. Coldren, and P.M. Petroff, Phys. Rev. Lett. **62**, 466 (1989).

[2] J.H. Neave, P.J. Dobson, B.A. Joyce, and J. Zhang, Appl. Phys. Lett. **47**, 100 (1985).

[3] T. Shitara, D.D. Vvedensky, M.R. Wilby, J. Zhang, J.H. Neave, and B.A. Joyce, Phys. Rev. B **46**, 6815 (1992); **46**, 6825 (1992).

[4] W.K. Burton, N. Cabrera, and F.C. Frank, Philos. Trans. R. Soc. London Ser. A **243**, 299 (1951).

[5] K. Voigtlaender and H. Risken, Appl. Phys. A **39**, 31 (1986); V. Fuenzalida and I. Eisele, J. Cryst. Growth **74**, 597 (1986).

[6] R. Ghez and S.S. Iyer, IBM J. Res. Dev. **32**, 804 (1988).

[7] A.K. Myers-Beaghton and D.D. Vvedensky, Phys. Rev. B **42**, 5544 (1990).

[8] A.K. Myers-Beaghton and D.D. Vvedensky, Phys. Rev. A **44**, 2457 (1991).

[9] V. Fuenzalida, Phys. Rev. B **44**, 10 835 (1991). Only the steady state is treated here but the generalization to the time-dependent case is straightforward.

[10] S. Harris, Phys. Rev. B **47**, 10 738 (1993).

[11] It is useful to note that the term "step flow" is usually used for a situation when no oscillations of a surface-sensitive probe (e.g., RHEED) are observed. An example of such experimental conditions taken from Ref. 3 for growth on a vicinal GaAs(001) surface misoriented by 2° toward the [010] direction is $T = 850$ K at $F = 0.20$ ML/s. However, large islands are still present on the surface under such conditions, but they are incorporated into advancing steps before they can nucleate a new layer. Therefore, a higher temperature or a lower incoming flux would be necessary to achieve "ideal" conditions for our model.

[12] This is the case for a (001) surface. Other choices are possible in which case the coefficients 8 ($= 2 \times 4$) and 4 in Eqs. (1) and (2) must be changed accordingly.

[13] S. Harris, Phys. Rev. B **49**, 2967 (1994).

[14] W. Tiller, *The Science of Crystallization: Microscopic Interfacial Phenomena* (Cambridge University Press, Cambridge, UK, 1991), Chap. 5.4; T. Risawa, Y. Arima, and T. Kuroda, J. Cryst. Growth **99**, 491 (1990).

[15] S. Harris, J. Cryst. Growth **97**, 319 (1989).

[16] H. Carslaw and J. Jaeger, *Heat Conduction in Solids* (Oxford University Press, Oxford, UK, 1957), Sec. 3.14.iv.

[17] This is similar to the procedure followed in approximating the linearized Boltzmann equation by the single relaxation time BGK (Bhatnagar, Gross, and Krook) equation. See, e.g., S. Harris, *Introduction to the Theory of the Boltzmann Equation* (Holt, Rinehart, and Winston, New York, 1971), Chap. 8.

[18] By this we mean that these effects are not included in the $m^{(0)}$ term indicated in R in Eq. (9). However, by retaining the $M^{(1)}$ in that term we are able, in part, to include the effects of disassociation in a self-consistent manner without having to carry out higher-order (and difficult) calculations.

[19] G. Ehrlich and F.G. Hudda, J. Chem. Phys. **44**, 1039 (1966).

[20] R.L. Schwoebel and E.J. Shipsey, J. Appl. Phys. **37**, 3682 (1966); R.L. Schwoebel, *ibid.* **40**, 614 (1969).

[21] J. Villain, J. Phys. I **1**, 19 (1991).

[22] H. Sakaki, M. Tanaka, and J. Yoshino, Jpn. J. Appl. Phys. **24**, L417 (1985).

[23] J.H. Neave, B.A. Joyce, P.J. Dobson, and N. Norton, Appl. Phys. A **31**, 1 (1983); F.J. Grunthaner, A. Madhukar, T.C. Lee, and R. Fernandez, J. Vac. Sci. Technol. B **3**, 1317 (1985); A. Yoshinaga, M. Fahy, S. Dosanjh, J. Zhang, J.H. Neave, and B.A. Joyce, Surf. Sci. **264**, L157 (1992).

[24] D.D. Vvedensky and S. Clarke, Surf. Sci. **225**, 373 (1990).

[25] L.-M. Peng and M.J. Whelan, Proc. R. Soc. London Ser. A **435**, 257 (1991).

[26] P. Šmilauer and D.D. Vvedensky, Phys. Rev. B **48**, 17 603 (1993).

[27] S. Kenny, M.R. Wilby, A.K. Myers-Beaghton, and D.D. Vvedensky, Phys. Rev. B **46**, 10 345 (1992).

[28] M.D. Johnson, C. Orme, A.W. Hunt, D. Graff, J. Sudijono, L.M. Sander, and B.G. Orr, Phys. Rev. Lett. **72**, 116 (1994).

[29] S. Harris, Phys. Rev. B (to be published).

[30] C.N. Luse, A. Zangwill, D.D. Vvedensky, and M.R. Wilby, Surf. Sci. Lett. **274**, L535 (1992).

[31] S. Stoyanov, Appl. Phys. A **50**, 349 (1990).

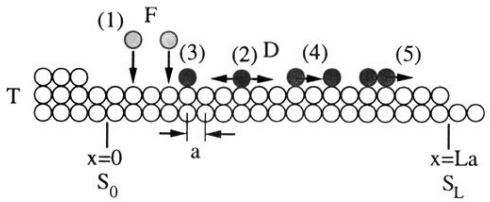

FIG. 1. Schematic picture of the processes considered in our model. Atoms are deposited (1) at a rate F onto the substrate with a lattice constant a held at a temperature T. They migrate (2) with the diffusion coefficient D and attach either to the preexisting steps (with probabilities given by the sticking coefficients S_0 and S_L) or form dimers (3), (4), which can subsequently disassociate (5). Two ways of a dimer creation, by a deposition of an incoming atom onto a nearest-neighbor site of a surface adatom (3) or by an encounter of two migrating adatoms (4), are shown.